

Unsteady evolution of localized unidirectional deep-water wave groups

Will Cousins and Themistoklis P. Sapsis*

Department of Mechanical Engineering, Massachusetts Institute of Technology, 77 Massachusetts Avenue, Cambridge, Massachusetts 02142, USA

(Received 22 October 2014; published 15 June 2015)

We study the evolution of localized wave groups in unidirectional water wave envelope equations [the nonlinear Schrödinger (NLSE) and the modified NLSE (MNLSE)]. These localizations of energy can lead to disastrous extreme responses (rogue waves). We analytically quantify the role of such spatial localization, introducing a technique to reduce the underlying partial differential equation dynamics to a simple ordinary differential equation for the wave packet amplitude. We use this reduced model to show how the scale-invariant symmetries of the NLSE break down when the additional terms in the MNLSE are included, inducing a critical scale for the occurrence of extreme waves.

DOI: [10.1103/PhysRevE.91.063204](https://doi.org/10.1103/PhysRevE.91.063204)

PACS number(s): 05.45.Yv, 47.35.Bb, 47.35.Fg

Understanding extreme events is critical due to the catastrophic damage they inflict. Important examples of extreme events are freak ocean waves [1,2], optical rogue waves [3], capsizing of ships [4], and extreme weather or climate events [5,6]. In this work we address the formation of freak or extreme waves on the surface of deep water. These waves have caused considerable damage to ships, oil rigs, and human life [7,8].

Extreme waves are rare and available data describing them are limited. Thus, analytical understanding of the physics of their triggering mechanisms is critical. One such mechanism is the Benjamin-Feir modulation instability of a plane wave to small sideband perturbations. This instability, which has been demonstrated experimentally, generates huge coherent structures by soaking up energy from the nearby field [9–12]. The ocean surface, however, is much more irregular than a simple plane wave. The Benjamin-Feir index (BFI), the ratio of surface amplitude to spectral width, measures the strength of the modulation instability in such irregular fields. For spectra with a large BFI, nonlinear interactions dominate, resulting in more extreme waves than Gaussian statistics would suggest. However, a large BFI does not provide precise spatiotemporal locations where extreme events might occur.

In large BFI regimes, spatially localized wave groups of modest amplitude focus, creating the extreme waves. Here we quantify the role of this spatial localization in extreme wave formation. In addition to providing insight into the triggering mechanisms for extreme waves, this analysis will allow the development of different spatiotemporal predictive schemes. Specifically, by understanding which wave groups are likely to trigger an extreme wave, one could identify when and where an extreme wave is likely to occur, in a manner similar to that of Cousins and Sapsis [13] for the Majda-McLaughlin-Tabak model [14]. By analyzing the evolution of spatially localized fields, the authors found a particular length scale that was highly sensitive for the formation of extreme events. By measuring energy localized at this critical scale, the authors reliably predicted extreme events for meager computational expense.

Two commonly used equations to model the envelope of a modulated carrier wave on deep water are the nonlinear Schrödinger equation (NLSE) and the modified NLSE (MNLSE) [15]. The focusing of localized groups is well understood for the NLSE (see the work of Adcock *et al.* [16,17] and Onorato *et al.* [18]). In this paper we study the less understood wave group focusing properties in the MNLSE model. That is, given a wave group of a particular amplitude and length scale, we determine if this group will focus and lead to an extreme wave.

We find two striking differences between the NLSE and MNLSE dynamics. First, due to a lack of scale invariance in the MNLSE, there is a minimal focusing length scale where wave groups below this scale do not focus. Second, the higher-order nonlinear terms of the MNLSE greatly inhibit focusing for some large amplitude groups. That is, there is a considerably smaller set of wave groups that would lead to an extreme event in the MNLSE in comparison to the NLSE. These features are critical for understanding realistic extreme waves, as the MNLSE is significantly more accurate in reproducing experimental results when compared with the NLSE [19,20].

We explain this difference in the NLSE and MNLSE focusing analytically by using a single mode, adaptive projection where the length scale of the mode is allowed to vary with time. We close this model by enforcing conservation of the \mathcal{L}^2 norm, which follows from the envelope equations. This drastically simplifies the relatively complex MNLSE partial differential equation (PDE), yielding a single ordinary differential equation (ODE) for the group amplitude. This reduced model agrees favorably with direct numerical simulations. Furthermore, the simplicity of this ODE model allows us to analytically explain various aspects of group evolution in the MNLSE, such as the existence of a minimal focusing length scale and the smaller family of focusing groups relative to the NLSE.

The NLSE [10] describes the evolution of the envelope of a slowly modulated carrier wave on the surface of deep water:

$$\frac{\partial u}{\partial t} + \frac{1}{2} \frac{\partial u}{\partial x} + \frac{i}{8} \frac{\partial^2 u}{\partial x^2} + \frac{i}{2} |u|^2 u = 0, \quad (1)$$

where u is the wave envelope, x is space, and t is time. In deriving the NLSE, the bandwidth is assumed to be narrow and the steepness is assumed to be small. Dysthe developed

*Corresponding author: sapsis@mit.edu

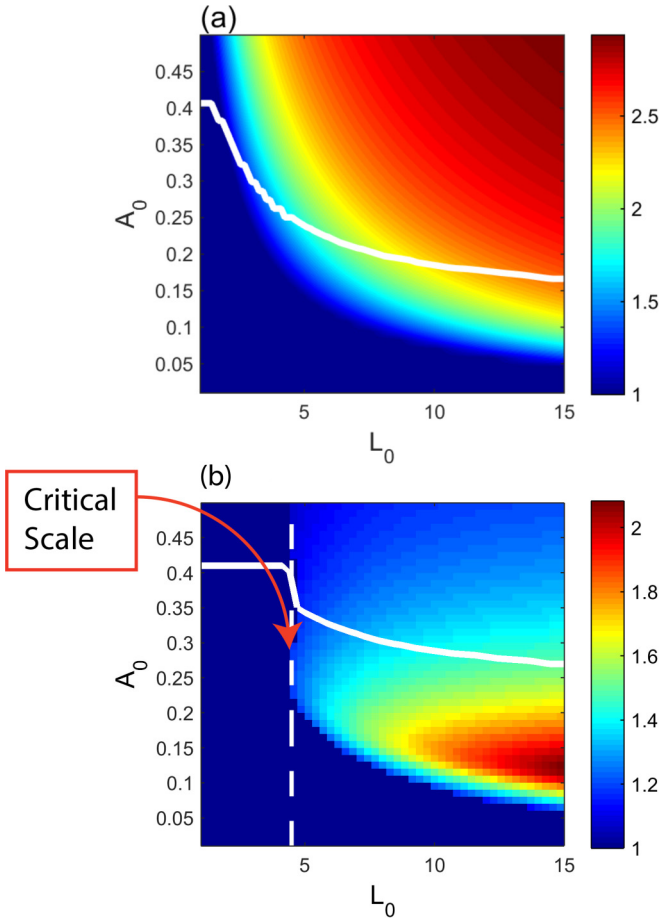


FIG. 1. (Color online) Ratio of the first spatiotemporal local maximum amplitude divided by the initial amplitude for the (a) NLSE and (b) MNLSE. In each figure, the solid white line denotes the onset of wave breaking in each respective PDE.

the MNLSE by incorporating higher-order terms [15]

$$\frac{\partial u}{\partial t} + \frac{1}{2} \frac{\partial u}{\partial x} + \frac{i}{8} \frac{\partial^2 u}{\partial x^2} - \frac{1}{16} \frac{\partial^3 u}{\partial x^3} + \frac{i}{2} |u|^2 u + \frac{3}{2} |u|^2 \frac{\partial u}{\partial x} + \frac{1}{4} u^2 \frac{\partial u^*}{\partial x} + iu \frac{\partial \phi}{\partial x} \Big|_{z=0} = 0, \quad (2)$$

where ϕ is the velocity potential, which may be expressed explicitly in terms of u by solving Laplace's equation [21]. To study the evolution of spatially localized groups, we use initial data of the form $u(x,0) = A_0 \text{sech}(x/L_0)$.

Using this family of initial conditions, we numerically compute the value of the first spatiotemporal local maximum of $|u|$. In Fig. 1 we display the value of this local maximum amplitude divided by the initial amplitude A_0 . This quantity is 1 when defocusing occurs and the amplitude decreases. Values of this ratio larger than 1 indicate that the associated group focuses, increasing in amplitude. We mention that Fig. 1(a) is similar to Fig. 1 of Onorato *et al.* [18], where a similar topic was studied for the NLSE.

For the NLSE, for each length scale there is an exact soliton solution with $A_0 = 1/\sqrt{2}L_0$, where the wave group shape is constant in time. If the initial amplitude is smaller than this solitonic amplitude, then the group broadens and its amplitude

decreases. If the initial amplitude is larger than this solitonic level, then the group focuses and increases in amplitude. This behavior is qualitatively the same for all length scales due to the scale invariance of the NLSE. Furthermore, the degree of focusing increases for larger amplitudes. That is, for all L_0 , A_{\max}/A_0 is an increasing function of A_0 .

We mention that a number of the cases pictured in Fig. 1 would yield breaking waves in a physical setting. Although the NLSE and MNLSE do not include such effects, the wave breaking threshold is typically taken to be $|u| = 0.4$. In Fig. 1 we include a white line showing where the maximally focused amplitude of the group exceeds 0.4. For (A_0, L_0) above this white line, the envelope equations are not physically accurate as they do not incorporate wave breaking. Although some of the pictured (A_0, L_0) do correspond to groups with breaking waves, there is a variety of groups below the breaking threshold where the NLSE and MNLSE differ considerably.

For the MNLSE, the situation is more complex [Fig. 1(b)]. Similar to the NLSE, for some (A_0, L_0) we do have an appreciable degree of focusing, thus the MNLSE possesses a mechanism for generating extreme waves. However, this behavior is *not* qualitatively the same for all length scales due to the additional nonlinear terms that lead to the breaking of scale invariance. In particular, there is a minimum focusing length scale where groups narrower than this length scale do not focus, regardless of how large their initial amplitude may be. Moreover, even when the length scale is larger, A_{\max}/A_0 is not a monotonically increasing function of A_0 . There is thus a finite range of amplitudes that lead to significant focusing. Furthermore, certain groups that do focus do so in a weaker sense compared to the NLSE. We reiterate that although some amplitudes in Fig. 1 exceed the well known physical maximum wave steepness of ≈ 0.4 [22], the NLSE and MNLSE wave group dynamics do show substantial differences for much lower, physically relevant amplitudes.

To develop an approximate model for the NLSE we approximate solutions as $u(x,t) = A(t) \text{sech}[(x - \frac{1}{2}t)/L(t)]$, which move at speed 1/2 as this is the group velocity for the NLSE. Applying the ansatz for u and projecting the equation to estimate $d|A|^2/dt$ results in a trivial equation

$$\frac{d|A|^2}{dt} = A^* \frac{dA}{dt} + A \frac{dA^*}{dt} = 0.$$

This equation is not helpful (although it is correct; we do observe the initial growth rate of groups to be zero in the full NLSE). We differentiate the NLSE (1) to obtain the second time derivative of $|u|^2$. We apply the ansatz for u , multiply the equation by the hyperbolic secant, and integrate over the real line. This is not sufficient to close the system as we have allowed both amplitude and length scale to vary with time. The NLSE conserves the integrated squared modulus of u , which implies $L(t) = L_0 |A_0/A(t)|^2$. Using this dynamical constraint, we obtain the following equation for $A(t)$:

$$\frac{d^2|A|^2}{dt^2} = \frac{K}{|A|^2} \left(\frac{d|A|^2}{dt} \right)^2 + \frac{3|A|^2(2|A|^2L^2 - 1)}{64L^2}, \quad (3)$$

where $K = (3\pi^2 - 16)/8$. We are interested in trajectories of (3) with initial conditions $|A(0)|^2 = A_0^2$ and $d|A|^2/dt|_{t=0} = 0$. Our reduced model has the correct, solitonic, fixed point

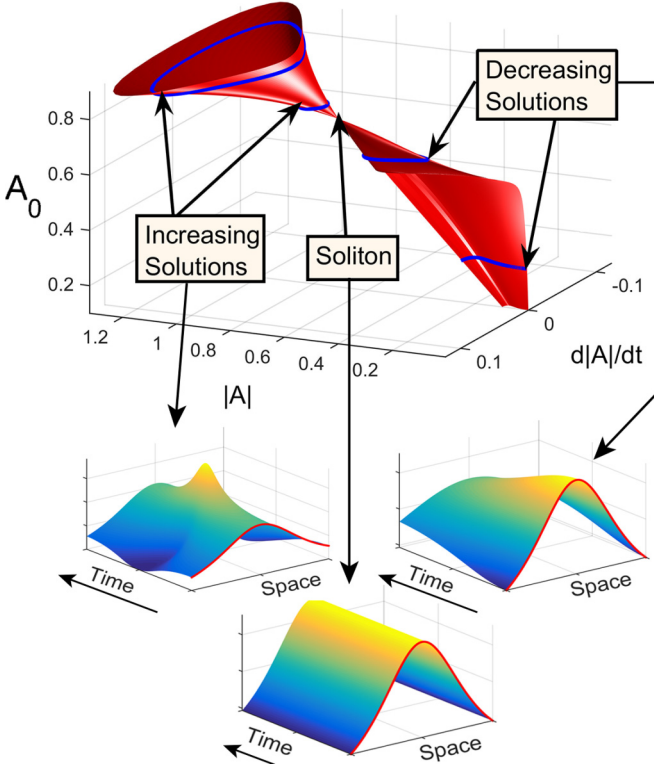


FIG. 2. (Color online) Surface described by solutions to the reduced order model (3) with various initial amplitudes $L_0 = 1$ along with predicted evolution for various wave groups.

$A_0 = 1/\sqrt{2}L_0$ and predicts focusing if the initial amplitude is larger than this solitonic value and decays if the initial amplitude is smaller (consistently with [16,17]). For a particular L_0 , the family of solutions to (3) describes a surface in the coordinates $(A_0, |A|, d|A|/dt)$ (although due to the scale invariance of the NLSE these surfaces are qualitatively the same for any $L_0 > 0$). We plot this phase surface in Fig. 2. The solitonic fixed point is clearly visible. Solutions with A_0 larger than the solitonic value grow to a new maximum and oscillate periodically between this new maximum and A_0 . Interestingly, values of A_0 just less than the solitonic amplitude decrease initially but oscillate periodically in time, never exceeding the initial amplitude (Adcock and Taylor made similar observations [16]). A comparison with a direct simulation of the NLSE reveals similar behavior, although for the NLSE we have energy leakage away from the main group.

Applying this methodology to the MNLSE is more complicated as there is an amplitude-dependent group velocity. To address this, we express the solution as $u(x,t) = A(t)\text{sech}[(x-ct)/L(t)]$, where c is an unknown constant group velocity. We first find the second temporal derivative of $|u|^2$ in a coordinate frame moving with group velocity c . Projecting the resulting equation gives

$$\begin{aligned} \frac{d^2|A|^2}{dt^2} &= \frac{K}{|A|^2} \left(\frac{d|A|^2}{dt} \right)^2 \\ &- c^2 \frac{3|A|^2}{2L^2} - c \frac{3|A|^2(-7|A|^2L^2 - 4L^2 - 1)}{8L^4} \end{aligned}$$

$$\begin{aligned} &- \frac{3|A|^2}{L^6} (980|A|^4L^4 + 832|A|^2L^4 + 392|A|^2L^2 \\ &+ 256L^4 + 160L^2 + 43), \end{aligned} \quad (4)$$

where again $L(t) = L_0|A_0/A(t)|^2$. We must also prescribe a value for c . Consider the envelope $|u|$ of a generic wave packet, where for each time t there is a single local maximum whose spatial position is given by $x = bt$. If we consider the evolution of $|u|$ along the ray $x' = ct$, we have that $|u(x' = ct, t)| < |u(x = bt, t)|$ if $c \neq b$. Thus, for wave group $|u|$ traveling with speed b , the growth of $|u|$ along the ray $x = ct$ is maximized (with respect to c) when we set $c = b$. To select c in the reduced-order model (4), we apply this criterion, choosing the value of c that maximizes the right-hand side of (4), which governs the growth of $|A|$. This gives

$$c = \frac{7A_0^2L_0^2 + 4L_0^2 + 1}{8L_0^2}. \quad (5)$$

As expected, c tends to the NLSE group velocity of $1/2$ as L_0 becomes large. Substituting (5) for c in (4) gives the following equation for $|A|^2$:

$$\begin{aligned} \frac{d^2|A|^2}{dt^2} &= \frac{K}{|A|^2} \left(\frac{d|A|^2}{dt} \right)^2 - \frac{3|A|^2}{2048L^6} (196|A|^4L^4 - 64|A|^2L^4 \\ &+ 168|A|^2L^2 + 32L^2 + 27). \end{aligned} \quad (6)$$

The reduced-order MNLSE (6) has a bifurcation at $L = \sqrt{14/4} + \sqrt{35/16} \approx 3.35$. If $L_0 < L^*$, the right-hand side of (6) will initially be negative, regardless of how large A_0 may be. Thus, groups with length scale less than L^* do not grow. This is precisely the behavior we observe in numerical simulations of the full MNLSE (Fig. 1). To illustrate these analytical results, we solve the reduced equation numerically for various L_0 and A_0 and display A_{\max}/A_0 in Fig. 3.

For $L_0 > L^*$, (6) has two fixed points. The amplitude will grow only when A_0 is *between* these two fixed points. Even for some focusing groups, the degree of focusing will be limited; the presence of the larger fixed point limits the amplitude

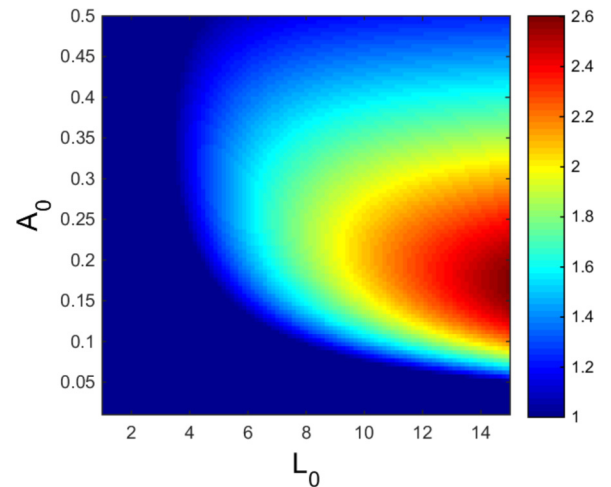


FIG. 3. (Color online) Maximal value of $A(t)$ relative to A_0 for solutions of the reduced order MNLSE model (6). This compares favorably direct numerical simulations of the MNLSE [Fig. 1(b)].

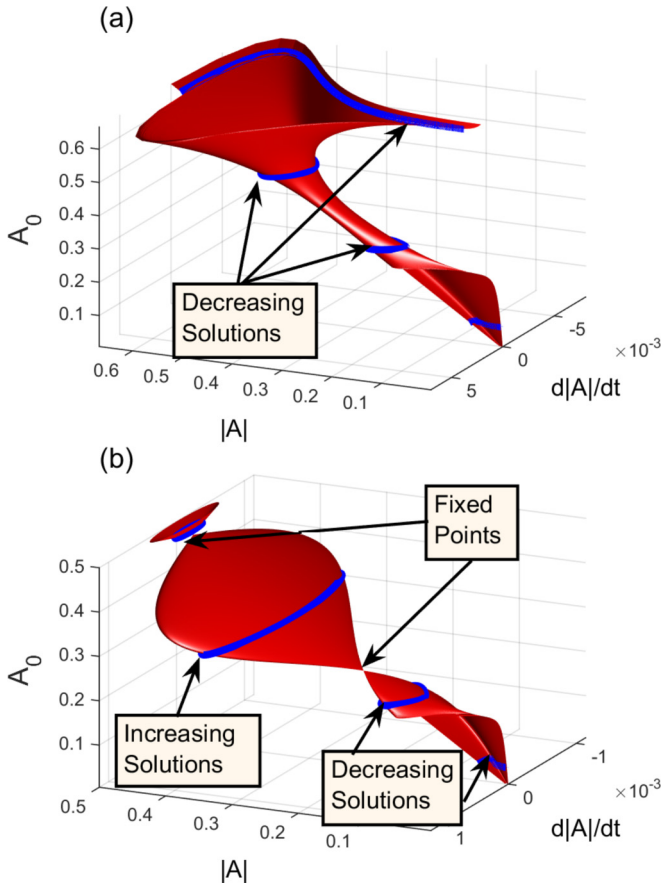


FIG. 4. (Color online) Phase surface diagrams for solutions to (6) with (a) $L_0 = 3$ and (b) $L_0 = 4$. (b) shows the emergence of two fixed points.

growth relative to the NLSE, agreeing with direct numerical simulations of the modified nonlinear Schrödinger PDE. Each of these two fixed points suggests an envelope soliton of the MNLSE. Although numerical simulations suggest that the lower-amplitude fixed point does correspond to a soliton, the larger-amplitude fixed point does not and is thus an artifact of the reduced-order model.

To illustrate the dynamics for the MNLSE, we display phase surfaces in Fig. 4 for $L_0 = 3$ and 4. For $L_0 = 3 < L^*$, all groups decay, with some groups oscillating periodically and others decaying monotonically. For $L_0 = 4 > L^*$, two fixed points emerge. Between these fixed points is the region of focusing, with groups in this region increasing in amplitude, but with a smaller increase compared with the NLSE.

Considering the surface elevation, the wave *crest height* amplification can be *larger* in the MNLSE due to higher-order terms in the formula for reconstructing the elevation from the envelope [23]. Crest-to-trough wave height amplification is lower in the MNLSE, agreeing with our observations of the dynamics of the envelope $|u|$ in this manuscript. The relevance

of the crest height vs crest-to-trough height depends on the particular application of interest.

In summary, we developed an approach for the analytical understanding of one-dimensional wave group evolution. Using a single-mode adaptive projection, we derived a simple ODE that mimics the dynamics of the underlying PDE remarkably well. The key of our approach allows the localized mode to adaptively adjust its length scale to respect the conservative properties of the PDE. The reduced-order model explains a number of salient scale-varying features of group evolution in the MNLSE.

Compared with existing methods, our approach provides a large amount of information while being simple to implement. For comparison, the BFI is simple to compute but does not provide the rich information of our approach. Methods based on the inverse scattering transform (IST) provide complete information but are complicated to implement [24–26]. Additionally, the IST is not applicable to two-dimensional wave dynamics where the governing equations are not integrable [27]. The approach presented here is similar in spirit to existing soliton perturbation approaches for the NLSE [28,29]. However, these approaches either consider only small perturbations about soliton solutions or require theoretical machinery unavailable for the MNLSE.

The main limitation of our approach is the assumption of a persistent hyperbolic-secant-shaped profile. In some cases, initial hyperbolic-secant-shaped profiles can become multihumped or asymmetric, violating our assumed profile shape. However, over short time scales the hyperbolic secant profile is nearly preserved. We mention that these short time scales correspond to physical time scales of a few minutes in a field with a spatial wavelength of 200 m (typical in the deep ocean).

We intend to apply this methodology to wave group evolution in the two-dimensional (2D) MNLSE and compare these dynamics with existing results for the 2D NLSE [17]. Moreover, this analysis will be fruitful in developing a scheme to predict extreme waves before they occur; we can use this analysis to determine which groups in an irregular random wave field are likely to focus and create an extreme wave. Our initial results suggest that our group-based analysis remains valid in this random wave field scenario, with groups appearing in these random fields evolving similarly to the predictions of the reduced-order models introduced in this work [30].

We also plan to use this approach to develop quantification schemes for the heavy tailed statistics of such intermittently unstable systems using a total probability decomposition [31]. Finally, this adaptive projection approach respecting invariant properties of the solution introduces a paradigm that will be useful for other systems involving energy localization [32,33].

The authors gratefully acknowledge support from the Naval Engineering Education Center Grant No. 3002883706 and ONR Grant No. N00014-14-1-0520.

[1] K. Dysthe, H. Krogstad, and P. Muller, *Annu. Rev. Fluid Mech.* **40**, 287 (2008).

[2] P. Muller, C. Garrett, and A. Osborne, *Oceanography* **18**, 66 (2005).

- [3] D. Solli, C. Ropers, P. Koonath, and B. Jalali, *Nature (London)* **450**, 1054 (2007).
- [4] E. Kreuzer and W. Sichertmann, *Comput. Sci. Eng.* **8**, 26 (2006).
- [5] J. Neelin, B. Lintner, B. Tian, Q. Li, L. Zhang, P. Patra, M. Chahine, and S. Stechmann, *Geophys. Res. Lett.* **37**, L05804 (2010).
- [6] A. J. Majda and B. Gershgorin, *Proc. Natl. Acad. Sci. USA* **107**, 14958 (2010).
- [7] S. Haver, in *Proceedings of Rogue Waves*, edited by M. Olagnon and M. Prevosto (Ifremer, Brest, 2004), pp. 1–8.
- [8] P. C. Liu, *Geofizika*. **24**, 57 (2007).
- [9] T. B. Benjamin and J. E. Feir, *J. Fluid Mech.* **27**, 417 (1967).
- [10] V. E. Zakharov, *J. Appl. Mech. Tech. Phys.* **9**, 190 (1968).
- [11] A. R. Osborne, M. Onorato, and M. Serio, *Phys. Lett. A* **275**, 386 (2000).
- [12] A. Chabchoub, N. P. Hoffmann, and N. Akhmediev, *Phys. Rev. Lett.* **106**, 204502 (2011).
- [13] W. Cousins and T. P. Sapsis, *Physica D* **280-281**, 48–58 (2014).
- [14] A. Majda, D. W. McLaughlin, and E. Tabak, *J. Nonlinear Sci.* **7**, 9 (1997).
- [15] K. B. Dysthe, *Proc. R. Soc. London Ser. A* **369**, 105 (1979).
- [16] T. Adcock and P. Taylor, *Proc. R. Soc. London Ser. A* **465**, 3083 (2009).
- [17] T. Adcock, R. Gibbs, and P. Taylor, *Proc. R. Soc. London Ser. A* **468**, 2704 (2012).
- [18] M. Onorato, A. Osborne, R. Fedele, and M. Serio, *Phys. Rev. E* **67**, 046305 (2003).
- [19] A. Goullet and W. Choi, *Phys. Fluids* **23**, 016601 (2011).
- [20] E. Lo and C. Mei, *J. Fluid Mech.* **150**, 395 (1985).
- [21] K. Trulsen and K. B. Dysthe, *Wave Motion* **24**, 281 (1996).
- [22] A. Toffoli, A. Babanin, M. Onorato, and T. Waseda, *Geophys. Res. Lett.* **37**, 33 (2010).
- [23] A. V. Slunyaev and V. Shrira, *J. Fluid Mech.* **735**, 203 (2013).
- [24] A. Slunyaev, *Eur. J. Mech. B* **25**, 621 (2006).
- [25] A. R. Osborne, M. Onorato, and M. Serio, *Proceedings of the 14th 'Aha Huliko'a Hawaiian Winter Workshop on Rogue Waves* (US Office of Naval Research, Honolulu, 2005).
- [26] A. Islas and C. Schober, *Phys. Fluids* **17**, 031701 (2005).
- [27] A. Osborne, *Nonlinear Ocean Waves & the Inverse Scattering Transform* (Academic, New York, 2010), Vol. 97.
- [28] A. L. Fabrikant, *Wave Motion* **2**, 355 (1980).
- [29] W. L. Kath and N. F. Smyth, *Phys. Rev. E* **51**, 1484 (1995).
- [30] W. Cousins and T. Sapsis (unpublished).
- [31] M. Mohamad and T. Sapsis (unpublished).
- [32] Y. Chung and P. M. Lushnikov, *Phys. Rev. E* **84**, 036602 (2011).
- [33] M. Erkintalo, Ph.D. thesis, Julkaisu-Tampere University of Technology, 2011.